Electronic Supplementary Material (ESI) for Materials Advances.

Supplementary Information: Copper-based core-shell metamaterials with ultra-broadband and reversible ENZ tunability

Anastasiia Zaleska, Alexey V. Krasavin, Anatoly V. Zayats, and Wayne Dickson

Department of Physics and London Centre for Nanotechnology, King's College London, Strand, London WC2R 2LS, United Kingdom

June 5, 2024

List of Figures

References

1. Lissberger, P. & Nelson, R. Optical properties of thin film Au-MgF2 cermets. *Thin Solid Films* **21,** 159–172 (Mar. 1974).
2. Pollard, R. J. *et al.* Optical Nonlocalities and Additional Waves in Epsilon-Near-Zero Metamaterials. *Physical Review Letters* **102,** 127405. ISSN: 0031-9007 (Mar. 2009).

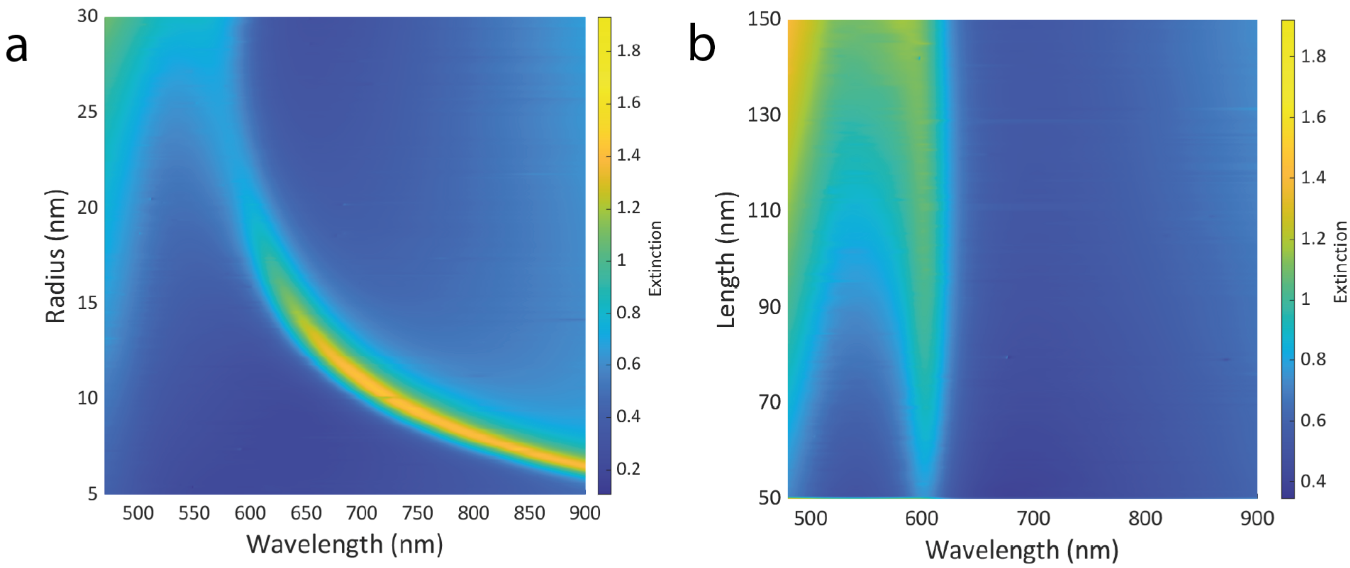

Figure S1: The calculated extinction spectra of copper nanorod array exposed in the air showing the effect of the rod (a) radius and (b) length on the optical properties of the metamaterial. The nanostructure with a fixed period of 85 nm, (a) a length of 100 nm and (b) a radius of 20 nm was illuminated under TM-polarised light at a 40°angle of incidence.

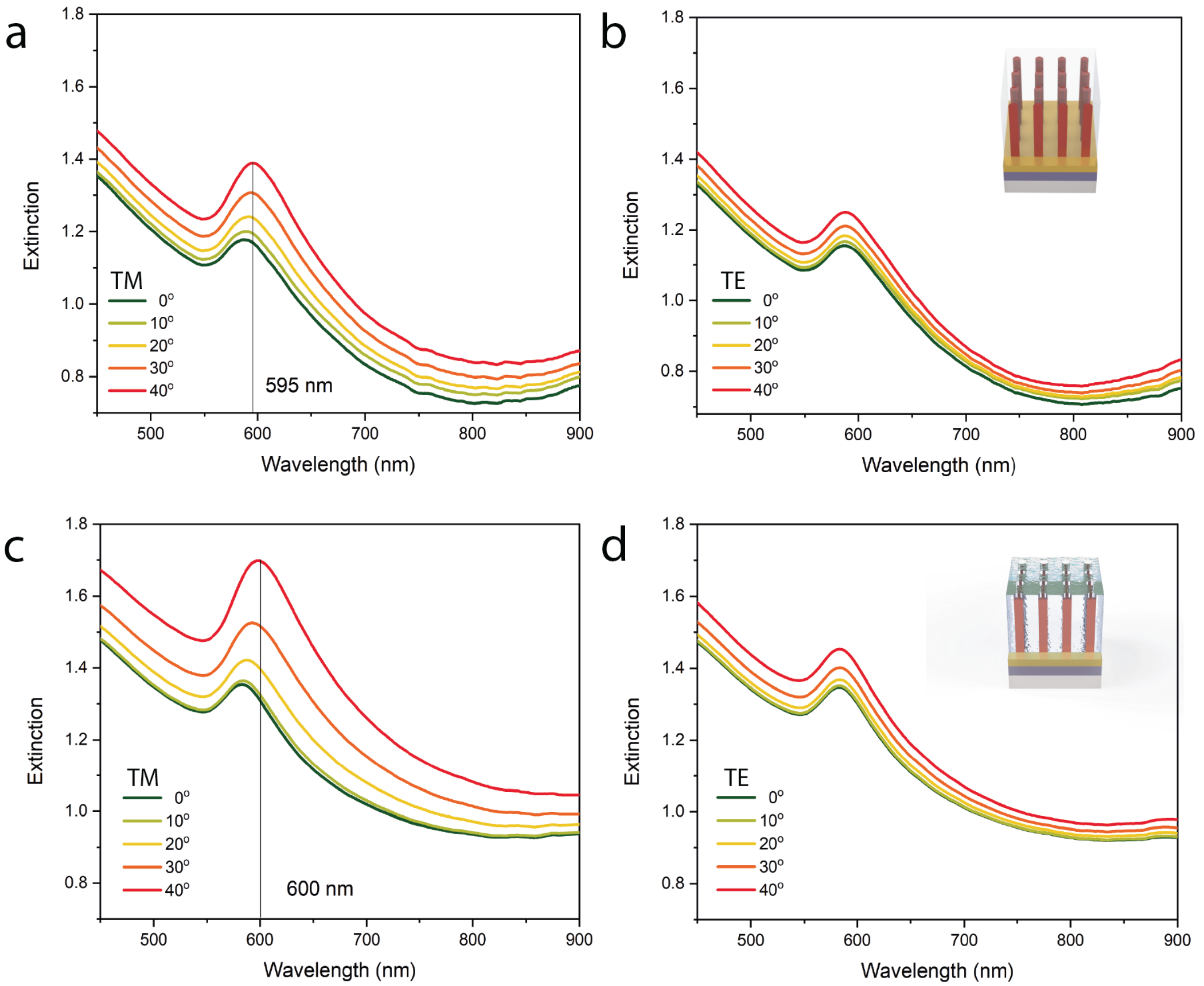

Figure S2: Measured extinction spectra of Cu nanorods exposed in air (a,b) and water (c,d) as a function of an angle of incident light illuminated with TM and TE polarisation. The metamaterials dimensions: a 20 nm radius, a 220 nm length and an 85 nm period.

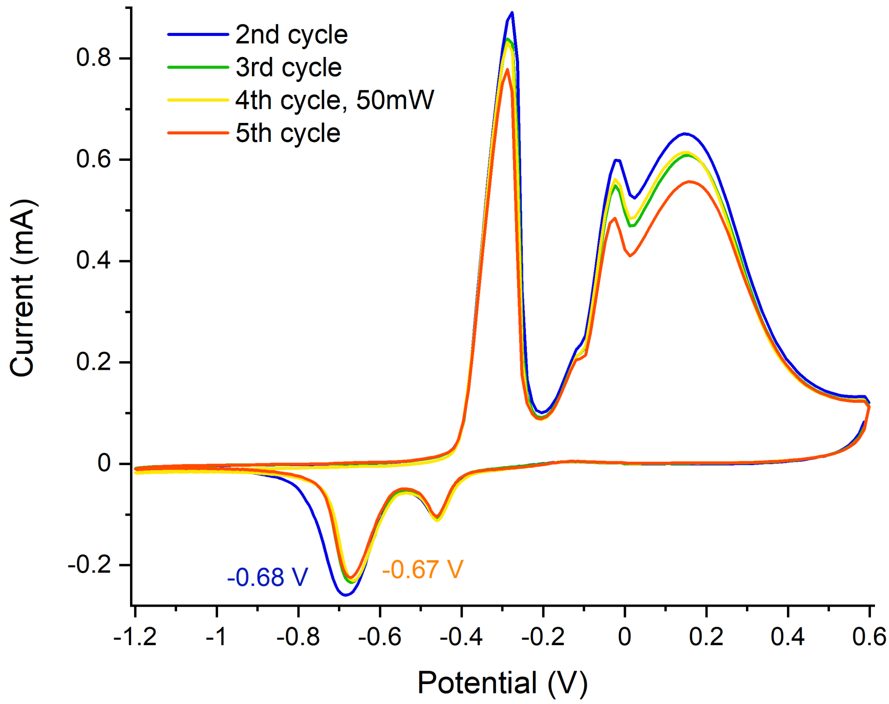

Figure S3: Cyclic voltammetry obtained with Cu nanorods in 0.15 M NaOH with scan rate of 0.01 Vs $^{-1}$ during five cycles. The precycle performed prior to these measurements is not shown.

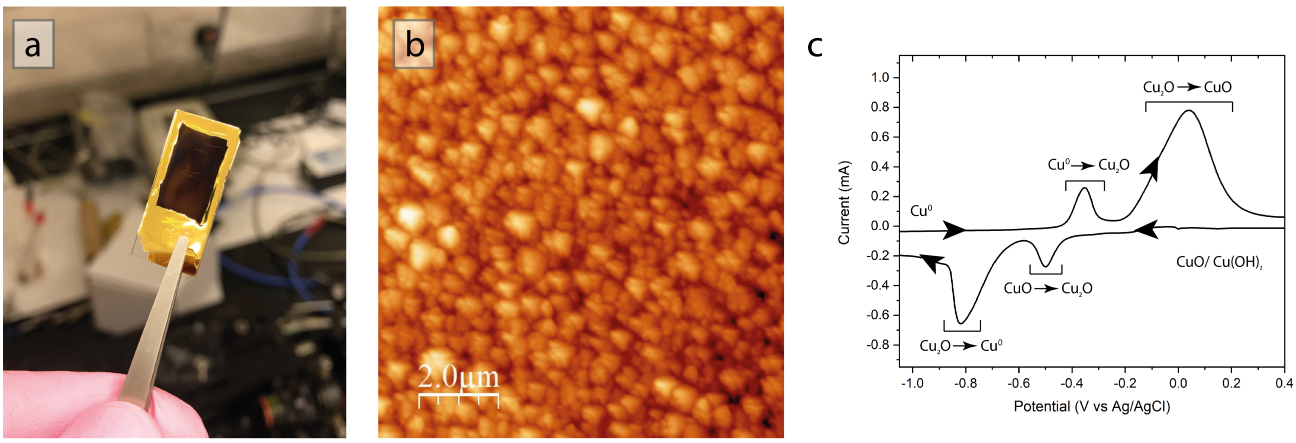

Figure S4: The formation of copper (I) oxide on a copper thin film surface after the anodisation process at -0.39 V in a 0.15 M NaOH solution: (a) photographic and (b) AFM image of the morphology of a copper film after the anodisation process. (c) Cyclic voltammetry of a Cu thin film on Au substrate performed in 0.15 M NaOH with a scan rate of 0.01 Vs $^{-1}$.

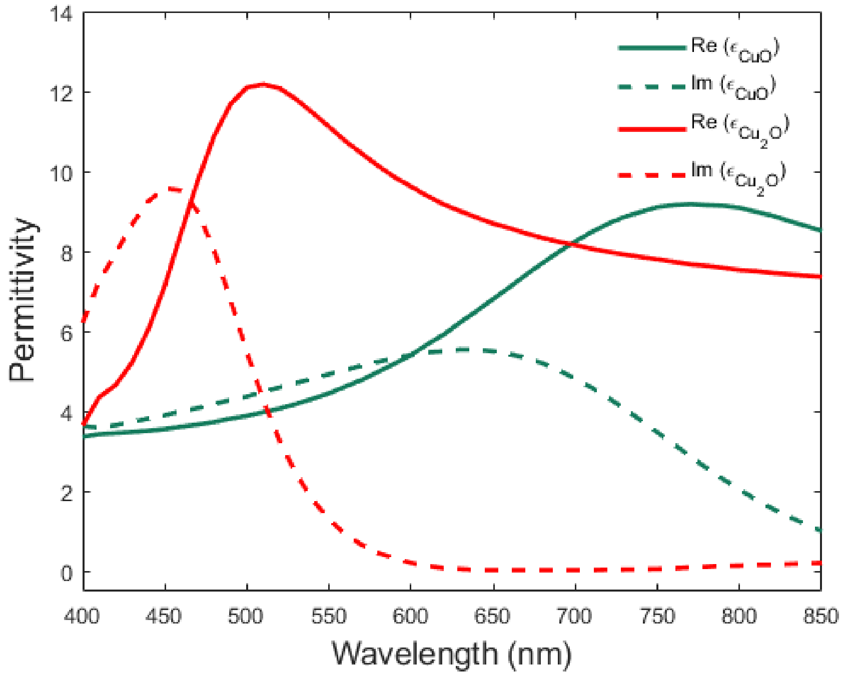

Figure S5: Spectral dependence of real and imaginary parts of permittivity for CuO and Cu_2O.

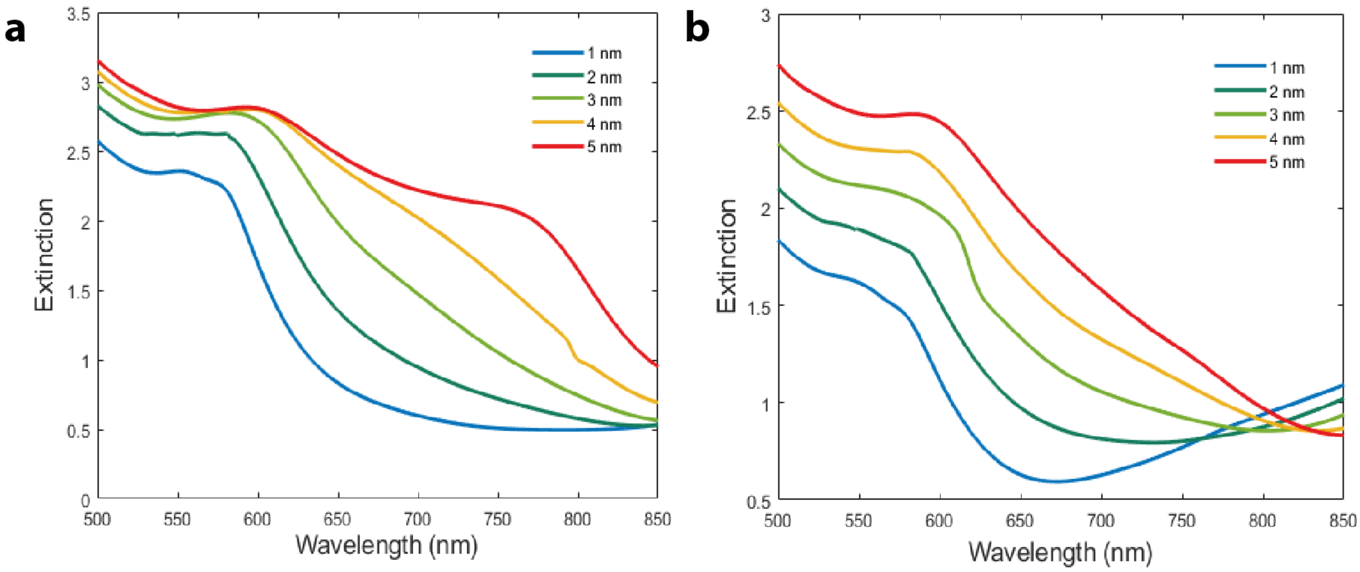

Figure S6: The simulated extinction spectra of the metamaterial as a function of the thickness of the CuO shell, formed on the copper nanorod surface, for the illumination with (a) TM- and (b) TE-polarised light at various angles of incidence.

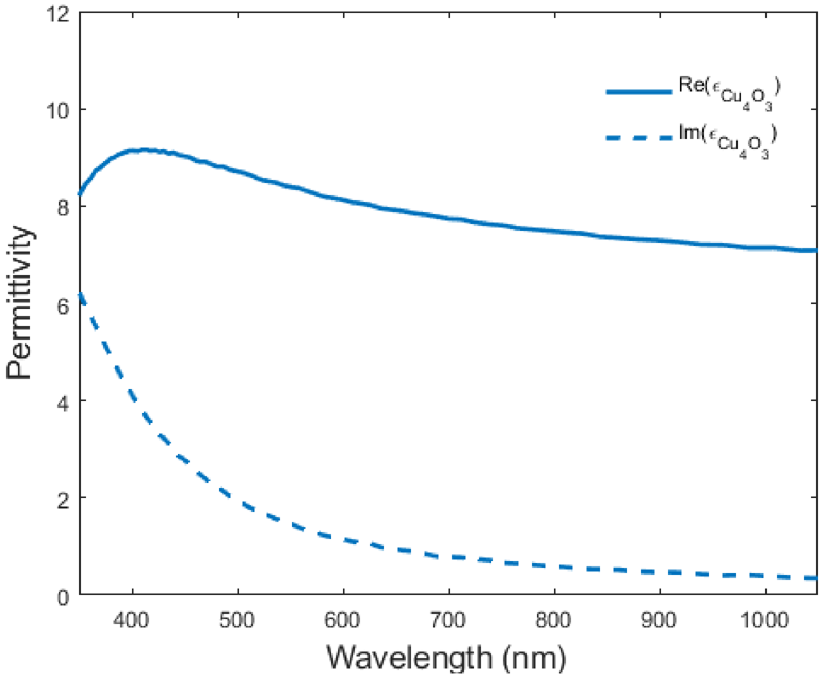

Figure S7: Spectral dependence of real and imaginary parts of permittivity for Cu_4O_3.

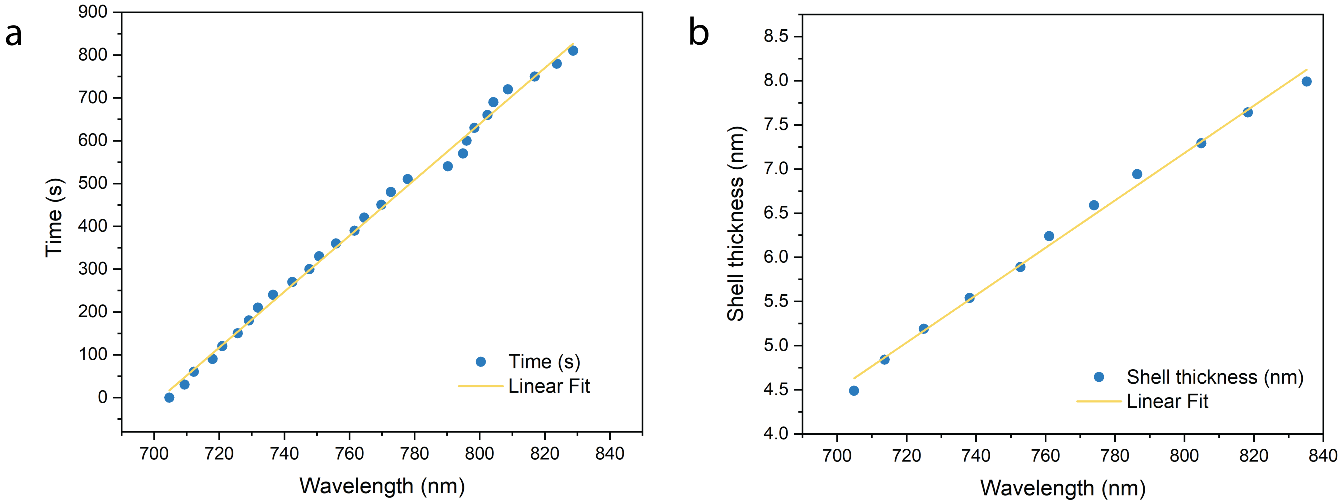

Figure S8: Estimation of the growth rate of the copper oxide shell. The spectral position of the ENZ peak is plotted as a function of (a) time during copper nanorod anodisation and (b) the thickness of the oxide shell from the numerical simulations. The approximate growth rate of the copper oxide shell was estimated by linear fits to both plots and found to be 0.23 nm/min.

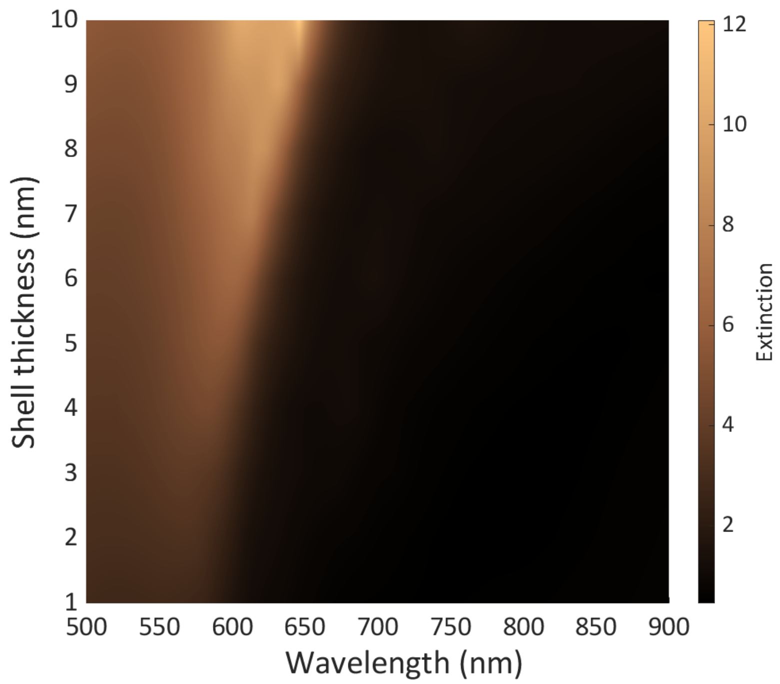

Figure S9: Map of simulated extinction spectra as a function of the shell thickness of Cu_2O with constant initial dimensions of copper nanorods. The initial geometrical parameters of copper nanorods are the following: 23 nm radius 180 nm length and 80 nm period.

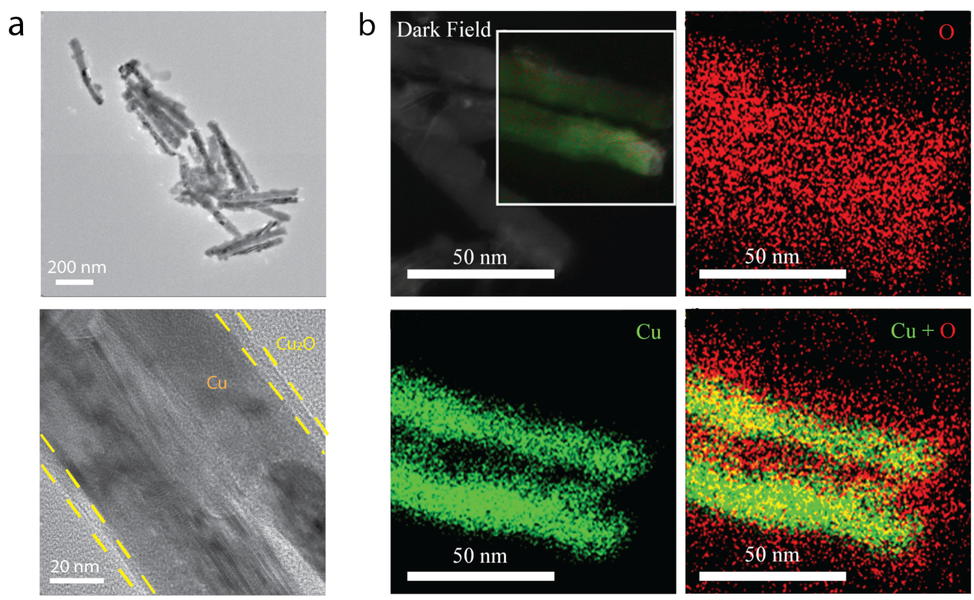

Figure S10: (a) TEM images of (top) a group of Cu-core/Cu_2O-shell nanorods detached from the metamaterial and (bottom) the high-resolution image of a single core-shell nanorod. (b) Dark-field TEM image of two core-shell nanorods (zoom into a) and respective EDS elemental mapping.

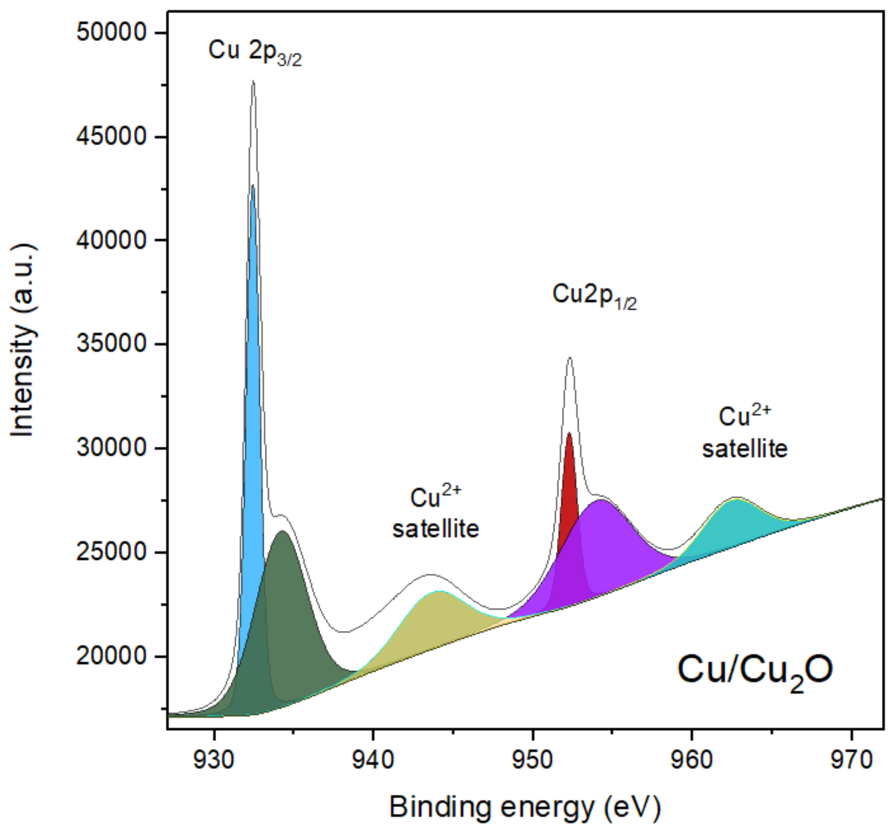

Figure S11: Cu 2p XPS core level spectra of copper nanorod surface after 4 minutes anodisation.

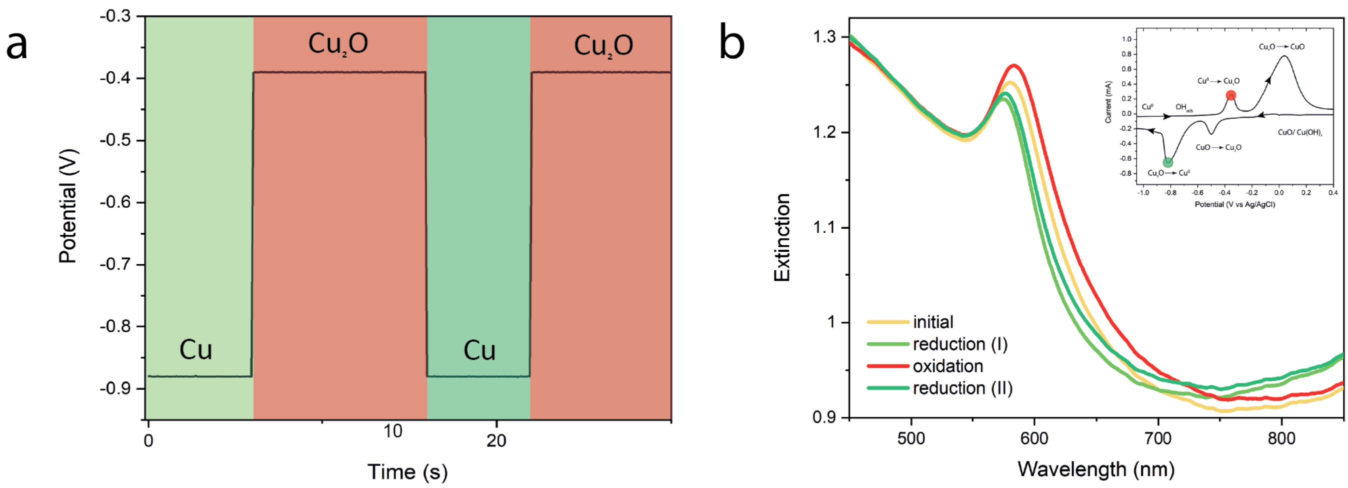

Figure S12: The optical response of the electrochemical switching between oxidation and reduction of the copper nanorod electrode at -0.39 V and -0.87 V vs. Ag/AgCl within 6 s and 10 s, respectively.

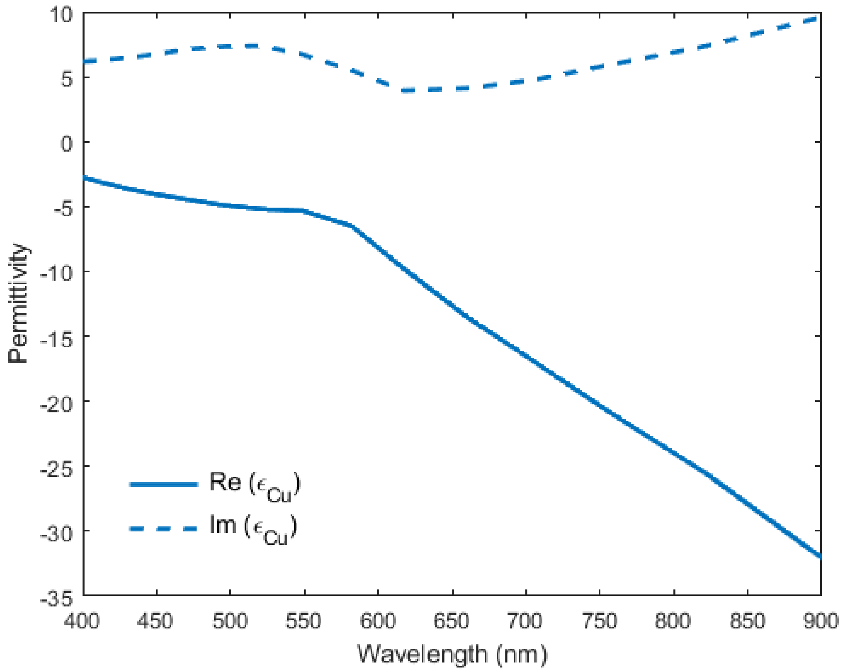

Figure S13: Spectral dependence of real and imaginary parts of permittivity for Cu (with introduced electron mean free path correction of 3.3 nm to take into account the highly polycrystalline nature of the nanorods [1, 2]).